Control Strategy for Two-Mode Hybrid Electric Vehicle by Using Fuzzy Controller

Jia-Shiun Chen, Hsiu-Ying Hwang

Abstract—Hybrid electric vehicles can reduce pollution and improve fuel economy. Power-split hybrid electric vehicles (HEVs) provide two power paths between the internal combustion engine (ICE) and energy storage system (ESS) through the gears of an electrically variable transmission (EVT). EVT allows ICE to operate independently from vehicle speed all the time. Therefore, the ICE can operate in the efficient region of its characteristic brake specific fuel consumption (BSFC) map. The two-mode powertrain can operate in input-split or compound-split EVT modes and in four different fixed gear configurations. Power-split architecture is advantageous because it combines conventional series and parallel power paths. This research focuses on input-split and compound-split modes in the two-mode power-split powertrain. Fuzzy Logic Control (FLC) for an internal combustion engine (ICE) and PI control for electric machines (EMs) are derived for the urban driving cycle simulation. These control algorithms reduce vehicle fuel consumption and improve ICE efficiency while maintaining the state of charge (SOC) of the energy storage system in an efficient range.

Keywords—Hybrid electric vehicle, fuel economy, two-mode hybrid, fuzzy control.

I. INTRODUCTION

THE internal combustion engine (ICE) is a widely used and well-developed technology, however, pollution and energy resource issues are associated with the ICE. Hybrid electric vehicles (HEVs) are an effective and common solution to these issues. Most manufacturers have been developing HEVs to improve the fuel economy and cost of their vehicles. Energy management and emission control for electric and IC engine power systems have been studied and developed for different types of hybrid systems [1]-[4]. Hendrickson et al. [5] introduced a two-mode hybrid (TMH) transmission for front-wheel drive vehicles developed by General Motors Powertrain. The two modes refer to two separate ranges of continuously variable engine-to-wheel speeds. The two modes are implemented by two planetary gear sets. As well as the two variable modes, the transmission also provides four forward fixed gear ratios. Their study presented the architecture and arrangement for a planetary gear set, electric motor, electrically variable transmission, and fixed gear. Several studies [6]-[8] have investigated a two-mode hybrid transmission for a full-size sport utility vehicle. The hybrid transmission architecture integrated two electro-mechanical power-split operating modes with four fixed gear ratios and mode operation strategies were explained.

In a hybrid electric vehicle, energy management is important because it can substantially affect the performance and size of the components of the vehicle. Therefore, an effective energy control strategy is essential for HEVs because it reduces fuel consumption, reduces emissions, and improves driving performance. Several control strategies have been implemented in HEVs [9]. Rule-based and fuzzy-based control strategies are commonly used in light and medium-sized HEVs. Rule-based control is simpler but less flexible than fuzzy-based control. Fuzzy-based control can identify and learn driver behaviors under various driving conditions. Both strategies are applicable for real-time control [10]. Although a dynamic programming (DP) solution can numerically optimize a specific drive-cycle [11], [12], stochastic dynamic programming (SDP) can optimize solutions for assumed road-load conditions with known probabilities [13]. In studies of heuristic rule-base methods [14], [15], experiments in fuzzy logic control (FLC) with an intelligent supervisory control strategy suggest that refined ICE speed transitions are also good candidates for implementation in control algorithms.

Power-split hybrid electric vehicles (HEVs) provide two power paths between the ICE and energy storage system (ESS) through gearing and compose an electrically variable transmission (EVT) [16]. The EVT allows the ICE to operate independently of vehicle speed. Therefore, the ICE can operate in the efficient region of its characteristic brake specific fuel consumption (BSFC) map. If the ICE produces more energy than that required by the driver, the extra energy is stored in the ESS for later usage. If the ICE cannot provide the energy required, the extra energy stored in the EM is used to meet the driver requirement.

Many studies have been done in ICE or hybrid vehicles; however, using fuzzy control to improve fuel economy for tow-mode hybrid vehicles has not been done yet. This research focused on input-split and compound-split modes of a two-mode hybrid powertrain. Fuzzy logic with optimal thresholds and transitions has been used to solve this design problem. Using feed forward control algorithms in a power-split HEV supervisory control strategy not only maintains the ICE operating points in an efficient region, but also maintains the state of charge (SOC) of ESS in optimal range.

Jia-Shiun Chen is with the Department of Vehicle Engineering, National Taipei University of Technology, Taipei 10608, Taiwan (phone: 886-2-27712171 Ext.3626; fax: 886-2-2731-4990; e-mail: chenjs@mail.ntut.edu.tw).

Hsiu-Ying Hwang is with the Department of Vehicle Engineering, National Taipei University of Technology, Taipei 10608, Taiwan (e-mail: hhwang@mail.ntut.edu.tw).

II. DYNAMIC MODELING OF FRONT-WHEEL DRIVE POWER-SPLIT GM HYBRID VEHICLE

Fig. 1 shows the main components of the TMH powertrain: the battery, IC engine, two braking clutches, three rotating transfer clutches, two motor-generators (MGs), and two planetary gear sets (P1 and P2). Table I shows the clutch engagement for each mode.
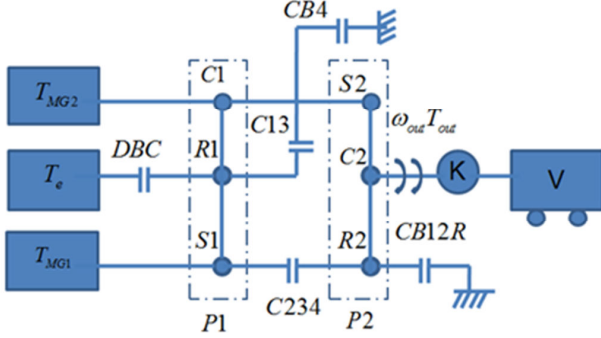

Fig. 1 Schematic layout of the Two-Mode HEV

TABLE I
CLUTCHES ASSOCIATED WITH MODE SELECTION

Mode	CB12R	C234	C13	CB4	DBC
EVT-1	On				
EVT-2		On			
FG-1	On		On		
FG-2	On	On			
FG-3		On	On		
FG-4		On		On	
Battery only	On				
Engine On/Off	On				On/Off

A. EVT-1 mode

In EVT-1 mode, input-split operation is achieved by locking the ring gear of P2 with clutch CB12R. The engine power is split by P1 while P2 works as fixed gear, which provides torque multiplication. In EVT-1, the speed and torque constraints are:

$$\omega_{MG1} = \frac{R_{R1}}{R_{S1}}\omega_E - \frac{(R_{R1} - R_{S1})}{R_{S1}}\frac{(R_{R2} + R_{S2})}{R_{S2}}\omega_{out} \tag{1}$$

$$\omega_{MG2} = \frac{(R_{R2} + R_{S2})}{R_{S2}}\omega_{out} \tag{2}$$

$$T_{MG1} = -\frac{R_{S1}}{R_{R1}}T_E \tag{3}$$

$$T_{MG2} = -\frac{R_{R1} + R_{S1}}{R_{R1}}T_E + \frac{R_{S2}}{(R_{R2} + R_{S2})}T_{out} \tag{4}$$

where ω_{MG1}, ω_{MG2}, ω_E, and ω_{out} are the MG1, MG2, ICE, and output shaft rotational velocities, respectively. The T_{MG1}, T_{MG2}, T_E, and T_{out} are the MG1, MG2, ICE, and output shaft torques, respectively. The R_{R1}, R_{S1}, R_{R2}, R_{S2} are the ring and sun gear radii of planetary gear sets P1 and P2, respectively.

B. EVT-2 Mode

In EVT-2 mode, compound-split operation is achieved by locking the ring gear of P2 to sun gear of P1 with clutch C234. The power is split by P1 at the input and combined by P2 at output. While operating in EVT-2, the constraining speed equations are:

$$\omega_{MG1} = \frac{R_{S2}R_{R1}}{(R_{R1}R_{R2} - R_{S1}R_{R2} - R_{S1}R_{S2})}\omega_E + \frac{(R_{R1} - R_{S1})(R_{R2} + R_{S2})}{(R_{R1}R_{R2} - R_{S1}R_{R2} - R_{S1}R_{S2})}\omega_{out} \tag{5}$$

$$\omega_{MG2} = \frac{R_{S2}R_{R1}}{(R_{R1}R_{R2} - R_{S1}R_{R2} - R_{S1}R_{S2})}\omega_E - \frac{R_{S1}(R_{R2} + R_{S2})}{(R_{R1}R_{R2} - R_{S1}R_{R2} - R_{S1}R_{S2})}\omega_{out} \tag{6}$$

The torque equations are

$$T_{MG1} = -\frac{R_{S1}}{R_{R1}}T_E + \frac{R_{R2}}{R_{R2} + R_{S2}}T_{out} \tag{7}$$

$$T_{MG2} = -\frac{R_{R1} - R_{S1}}{R_{R1}}T_E + \frac{R_{S2}}{(R_{R2} + R_{S2})}T_{out} \tag{8}$$

C. 1st Fixed Gear (FG-1)

The P1 is locked by C13, which allows direct connection to the sun gear of P2, and the ring gear of P2 is held stationary by CB12R, which provides a speed reduction. The FG-1 mode improves vehicle acceleration. In this mode, the speed and torque constraints are:

$$\omega_E = \omega_{MG1} = \omega_{MG2} = \frac{R_{R2} + R_{S2}}{R_{S2}}\omega_{out} \tag{9}$$

$$T_{out} = \left(\frac{R_{R2} + R_{S2}}{R_{S2}}\right)(T_E + T_{MG1} + T_{MG2}) \tag{10}$$

D. 2nd Fixed Gear (FG-2)

The FG-2 mode, which allows a smooth transient between EVT-1 and EVT-2, is the synchronous shift mode used by disengaging either C13 or C234, which are enabled by one of the EVT modes. The FG-2 occurs at the "mechanical point", and MG1 is stationary regardless of the operating condition. In FG-2 mode, the planetary gear set constraints result in speed and torque constraints of

$$\omega_E = \frac{(R_{R1} - R_{S1})}{R_{R1}}\frac{(R_{R2} + R_{S2})}{R_{S2}}\omega_{out} \tag{11}$$

$$\omega_{MG1} = 0 \tag{12}$$

$$\omega_{MG2} = \frac{(R_{R2} + R_{S2})}{R_{S2}}\omega_{out} \tag{13}$$

$$T_{out} = \frac{(R_{R1} - R_{S1})(R_{R2} + R_{S2})}{R_{R1}R_{S2}}T_E + \frac{(R_{R2} + R_{S2})}{R_{S2}}T_{MG2} \tag{14}$$

E. 3rd Fixed Gear (FG-3)

To improve hill climbing and towing capability, FG-3 allows the wheels to be driven directly by the IC engine. Both P1 and P2 planetary gear sets are locked by engaging C234 and C13. The FG-3 mode speed and torque constraints derived from the planetary gear sets constraints are

$$\omega_E = \omega_{MG1} = \omega_{MG2} = \omega_{out} \qquad (15)$$

$$T_{out} = (T_E + T_{MG1} + T_{MG2}) \qquad (16)$$

F. 4th Fixed Gear (FG-4)

When the P1 ring gear is locked by engaging C234 and the sun gear of P2 is held stationary by CB4, one overdrive fixed gear is enabled. The FG-4 mode operates at the second "mechanical point" of GM TMH architecture. This mode is best for constant vehicle speed cruising. The MG2 does not rotate, and no energy conversion loses is experienced by EM. Speed and torque constraints are:

$$\omega_E = \frac{R_{S1}(R_{R2} + R_{S2})}{R_{R1}R_{R2}} \omega_{out} \qquad (17)$$

$$\omega_{MG1} = \frac{R_{R2} + R_{S2}}{R_{R2}} \omega_{out} \qquad (18)$$

$$\omega_{MG2} = 0 \qquad (19)$$

$$T_{out} = \frac{R_{S1}(R_{R2} + R_{S2})}{R_{R1}R_{R2}} T_E + \frac{R_{R2} + R_{S2}}{R_{R2}} T_{MG1} \qquad (20)$$

To reduce power loss and increase efficiency, the power-split HEV uses two modes and four fixed gear configurations [11]. Smooth shifting mode at "mechanical points" prevent reversed power flow in MG1 and MG2 while remains engine speed at constant speed regardless vehicle speed, as shown in Fig. 2.
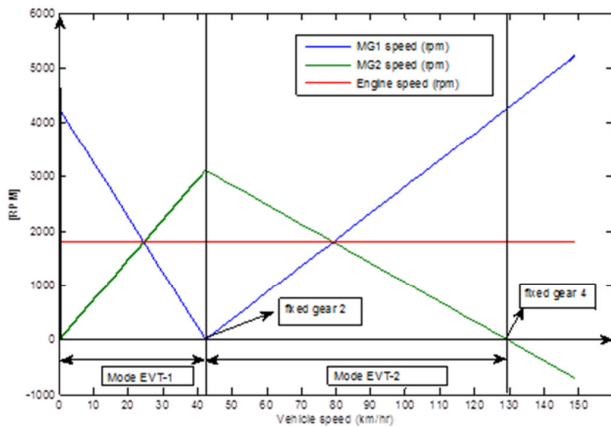

Fig. 2 Shifting EVT modes with engine speed at 1800 rpm

III. IMPLEMENTABLE CONTROL DESIGN OF THE TWO-MODE POWER-SPLIT GM HYBRID VEHICLE

A. Dynamic Equation Matrixes

A two-mode power-split system involves planetary gears and clutches and has different kinematic relationship between the gear modes. Two different sets of dynamic equations were derived to represent the model of the two CVT modes, and gear shifting between these two modes was modeled as switching between these two models.

1. EVT-1 Mode

Fig. 3 shows the free body diagram of the mechanical path for EVT-1 mode. The planetary gear sets are represented by two levers in the middle of the diagram. The R_{R1}, R_{S1} and R_{R2}, R_{S2} represent the ring gear and sun gear radii of P1 and P2, respectively. The F_1 and F_2 represent the internal forces between the pinion gears and the sun gear or ring gear of P1 and P2. Dynamic equations are expressed in the matrix below

$$\begin{bmatrix} \dot{\omega}_E \\ \dot{\omega}_{out} \\ \dot{\omega}_{MG1} \\ \dot{\omega}_{MG2} \\ F_1 \\ F_2 \end{bmatrix} = \begin{bmatrix} I_E + I_{R1} & 0 & 0 & 0 & R_{R1} & 0 \\ 0 & I_{C2} + \frac{r_{tire}^2}{K^2}m & 0 & 0 & 0 & -R_{R2} - R_{S2} \\ 0 & 0 & I_{MG1} + I_{S1} & 0 & -R_{S1} & 0 \\ 0 & 0 & 0 & I_{MG2} + I_{C1} + I_{S2} & -R_{R1} + R_{S1} & R_{S2} \\ R_{R1} & 0 & -R_{S1} & -R_{R1} + R_{S1} & 0 & 0 \\ 0 & -R_{R2} - R_{S2} & 0 & R_{S2} & 0 & 0 \end{bmatrix}^{-1} \begin{bmatrix} T_E \\ \frac{\sum F_r r_{tire}}{K} \\ T_{MG1} \\ T_{MG2} \\ 0 \\ 0 \end{bmatrix} \qquad (21)$$

where T_{MG1}, ω_{MG1}, and I_{MG1} are the MG1 torque, speed, and inertia, respectively. The K, r_{tire}, F_r, and m are the final drive ratio, tire radius, tire tractive force, and vehicle mass, respectively.
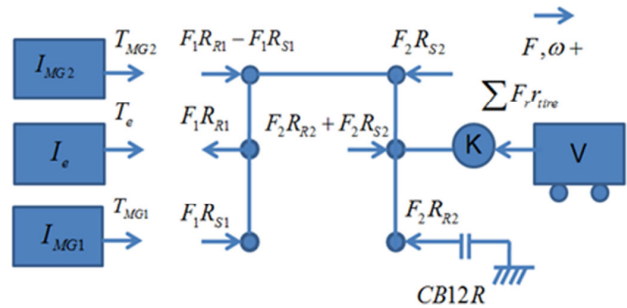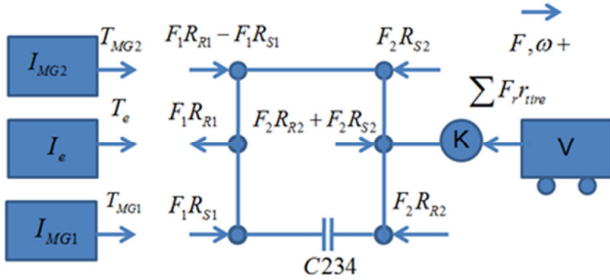

Fig. 3 Free body diagram of the ECT-1 mode powertrain

The output torque includes only the longitudinal dynamics,

$$-\frac{\sum F_r}{K} r_{tire} = (I_{C2} + \frac{r_{tire}^2}{K^2}m)\dot{\omega}_{out} - F_2(R_{R2} + R_{S2}) \qquad (22)$$

2. EVT-2 Mode

In the EVT-2 mode (compound-split mode) when MG1 speed reaches zero and C234 clutch is engaged, shifting mode occurs at the second fixed gear. The CB12R is then released, and Fig. 4 shows that the ring gear of P2 rotates at the same speed as the sun gear P1. The same procedure used in EVT-1

mode is used to derive the governing equations, and the equation matrix is

$$
\begin{bmatrix} \dot{\omega}_E \\ \dot{\omega}_{out} \\ \dot{\omega}_{MG} \\ \dot{\omega}_{MG} \\ F_1 \\ F_2 \end{bmatrix} = \begin{bmatrix} I_E+I_{R1} & 0 & 0 & 0 & R_{R1} & 0 \\ 0 & I_{C2}+\frac{r_{tire}^2}{K^2}m & 0 & 0 & 0 & -R_{S2}-R_{S2} \\ 0 & 0 & I_{MG}+I_{S1}+I_{R2} & 0 & -R_{S1} & R_{R2} \\ 0 & 0 & 0 & I_{MG}+I_{C1}+I_{S2} & -R_{R1}+R_{S1} & R_{S2} \\ R_{R1} & 0 & -R_{S1} & -R_{R1}+R_{S1} & 0 & 0 \\ 0 & -R_{R2}-R_{S2} & R_{R2} & R_{S2} & 0 & 0 \end{bmatrix}^{-1} \begin{bmatrix} T_E \\ \frac{\sum Fr_{tire}}{K} \\ T_{MG} \\ T_{MG} \\ 0 \\ 0 \end{bmatrix} \quad (23)
$$

Fig. 4 Free body diagram of the EVT-2 mode powertrain

These two operating modes can be switched between each other by controlling synchronized clutch shift [15]. Synchronization is achieved by controlling the speed of the electric machines.

B. Design of IC Engine Torque and Speed

The fuzzification procedure transforms crisp values into membership grades for linguistic terms of fuzzy sets. The membership function associates a grade with each linguistic term. The linguistic description provided by the expert can generally be broken into several parts. "Linguistic variables" describe each of the time-varying fuzzy controller inputs and outputs. The ICE torque and speed were designed according to load torque, vehicle speed, and SOC.
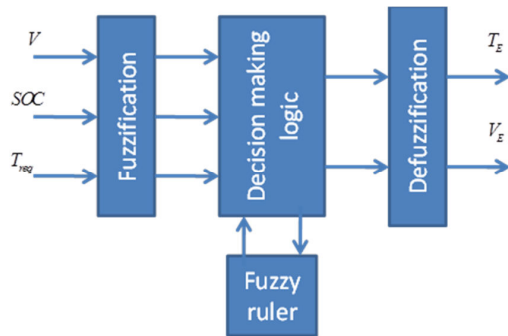

Fig. 5 Configuration of the fuzzy controller

1. Input Signals

Inputs signals included vehicle speed, SOC, and vehicle load torque. Vehicle speed was defined as 4 fuzzy variables: "vs", "m", "h", and "vh", as shown in Fig. 6. SOC was defined as 4 fuzzy variables: "s", "opt", "h", and "vh", as shown in Fig. 7. Fig. 8 shows that load torque was defined using 5 fuzzy variables: vs, s, m, h, and vh.
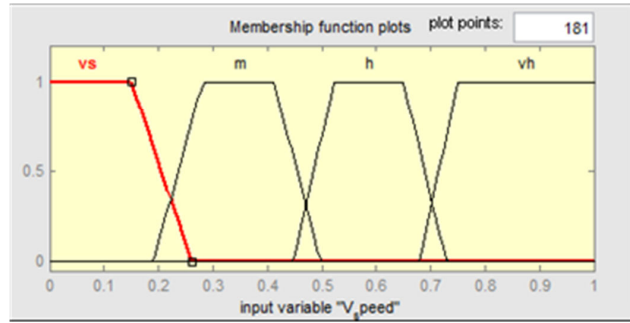

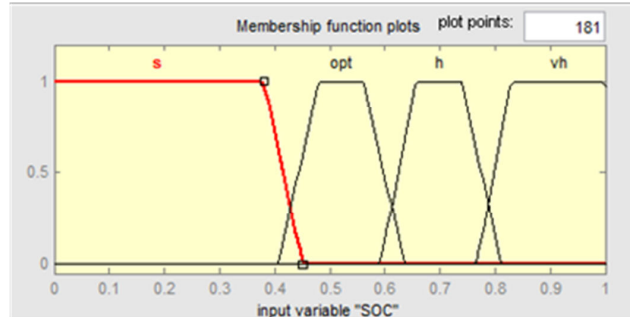Fig. 6 Membership function of vehicle speed
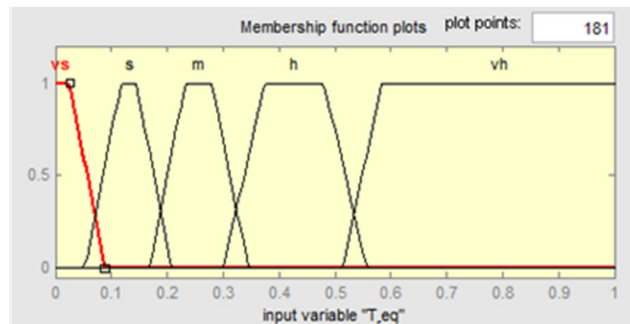

Fig. 7 Membership function of SOC

Fig. 8 Membership function of load torque

a) Output Signals

Outputs signals included engine torque and engine speed. Engine torque was defined as 5 fuzzy variables: "vs", "s", "opt_s", "opt_h", "h", as shown in Fig. 9. Engine speed was defined as 5 fuzzy variables: "s", "m", "opt_s", "opt_h", "h", as shown in Fig. 10.
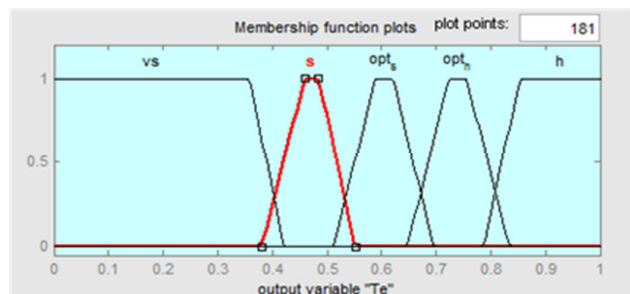

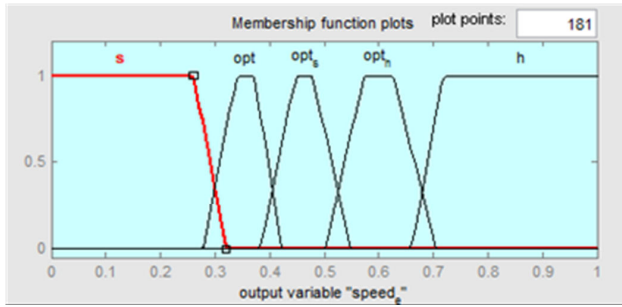
Fig. 9 Membership function of engine torque

Fig. 10 Membership function of engine speed

TABLE II
PART OF FUZZY LOGIC SET RULES

Vehicle speed	SOC	Load torque	Engine torque	Engine speed
vs	s	vs	Opt$_s$	Opt$_s$
vs	s	m	Opt$_h$	Opt$_h$
m	s	s	Opt$_s$	Opt$_s$
m	opt	m	Opt$_s$	Opt$_s$
h	s	vh	h	h
h	h	m	s	Opt$_s$
......				

b) Rule Base

The rule table included approximately 80 rules. Table II shows one part of the rule table.

c) Defuzzification

The resulting fuzzy set must be converted to single number to represent the control torque and speed signals for the IC engine. The MATLAB Simulink uses center of gravity defuzzifier method.

$$y^* = \frac{\int v_\alpha \mu_B(y) y \, dy}{\int v_\alpha \mu_B(y) \, dy} \tag{24}$$

d) Engine On/Off Algorithm

Engine on/off state was judged by mode state, vehicle speed, and SOC signals. In mode 2, the engine is turned on. In mode 1, the SOC turns the engine on or off at certain vehicle speeds. When the SOC exceeds 0.6, the engine turns on and off at high speeds to avoid over-discharging or over-charging the batteries.

C. EVT-1 Mode

From dynamic equations, there are only two independent state variables: engine speed and vehicle speed. Two control inputs are MG1 torque and MG2 torque, and IC engine torque depends on road load, which is determined by rolling resistance, wind resistance, and grading resistance torques.

The dynamic equations are reconstructed to find MG1 and MG2 torque as follows:

EVT-1 Mode:

$$\begin{bmatrix} \hat{T}_{MG1} \\ \hat{T}_{MG1} \end{bmatrix} = A \begin{bmatrix} K_P(\hat{\omega}_{E\_command} - \omega_E) + K_I \int_0^t (\hat{\omega}_{E\_command} - \omega_E) dt \\ K_P(\hat{\omega}_{V\_command} - \omega_V) + K_I \int_0^t (\hat{\omega}_{V\_command} - \omega_V) dt \end{bmatrix} + B \begin{bmatrix} \hat{T}_E \\ \dfrac{\sum \hat{F}_r}{K} r_{tire} \end{bmatrix} \tag{25}$$

where

$$A_{11} = \frac{R_{S1}}{R_{R1}}(I_E + I_{R1}) + (I_{MG1} + I_{S1})R_{R1}$$

$$A_{12} = -(I_{MG1} + I_{S1})(R_{R1} - R_{S1})\left(\frac{R_{S2} + R_{R2}}{R_{S2}}\right)$$

$$A_{21} = \frac{(I_{MG1} + I_{S1})(R_{R1} - R_{S1})}{R_{R1}}$$

$$A_{22} = \frac{R_{S2}\left(I_{C2} + \dfrac{r_{tire}^2}{K^2}m\right)}{R_{R2} + R_{S2}} + (I_{MG2} + I_{C1} + I_{S2})\frac{R_{R2} + R_{S2}}{R_{S2}}$$

$$B = \begin{bmatrix} -\dfrac{R_{S1}}{R_{R1}} & 0 \\ -\dfrac{(R_{R1} - R_{S1})}{R_{R1}} & \dfrac{R_{S2}}{(R_{R2} + R_{S2})} \end{bmatrix}$$

EVT-2 Mode:

$$\begin{bmatrix} \hat{T}_{MG} \\ \hat{T}_{MG} \end{bmatrix} = C \begin{bmatrix} K_P(\hat{\omega}_{E\_command} - \omega_E) + K_I \int_0^t (\hat{\omega}_{E\_command} - \omega_E) dt \\ K_P(\hat{\omega}_{V\_command} - \omega_V) + K_I \int_0^t (\hat{\omega}_{V\_command} - \omega_V) dt \end{bmatrix} + D \begin{bmatrix} \hat{T}_E \\ \dfrac{\sum \hat{F}_r}{K} r_{tire} \end{bmatrix} \tag{26}$$

where

$$C_{11} = \frac{R_{S1}}{R_{R1}}(I_E + I_{R1}) + \frac{(I_{MG1} + I_{S1} + I_{R2})R_{R1}R_{S2}}{R_{S1}R_{S2} - R_{R2}(R_{R1} - R_{S1})}$$

$$C_{12} = -\frac{(I_{MG1} + I_{S1} + I_{R2})(R_{R1} - R_{S1})(R_{R2} + R_{S2})}{R_{S1}R_{S2} - R_{R2}(R_{R1} - R_{S1})} + \frac{R_{R2}\left(I_{C2} + \dfrac{r_{tire}^2}{K^2 m}\right)}{(R_{R2} + R_{S2})}$$

$$C_{21} = -\frac{(I_{MG1} + I_{S1})(R_{R1} - R_{S1})}{R_{R1}} - \frac{R_{R1}R_{R2}(I_{MG2} + I_{C1} + I_{S2})}{R_{S1}R_{S2} - R_{R2}(R_{R1} - R_{S1})}$$

$$C_{22} = \frac{R_{S1}(I_{MG2} + I_{C1} + I_{S2})(R_{R2} + R_{S2})}{R_{S1}R_{S2} - R_{R2}(R_{R1} - R_{S1})} + \frac{R_{S2}\left(I_{C2} + \dfrac{r_{tire}^2}{K^2 m}\right)}{(R_{R2} + R_{S2})}$$

$$D = \begin{bmatrix} -\dfrac{R_{S1}}{R_{R1}} & \dfrac{R_{R2}}{R_{R2} + R_{S2}} \\ -\dfrac{(R_{R1} - R_{S1})}{R_{R1}} & \dfrac{R_{S2}}{R_{R2} + R_{S2}} \end{bmatrix}$$

$(\hat{\omega}_{E\_command} - \omega_E)$ and $(\hat{\omega}_{V\_command} - \omega_V)$ are small enough, and the engine speed difference is smaller than 1000 rpm in each time step Δt. Then, the control gains, K_P and K_I, are selected, and MG torques, T_{MG1} and T_{MG2}, are received from equations.

IV. SIMULATION RESULTS AND ANALYSES

All models were built in Matlab/Simulink environment. The vehicle model was based on a GM Impala, and Table III shows the HEV model parameters. All models are simulated in Urban Dynamometer Driving Schedule (UDDS), which refers to a dynamometer test of fuel economy mandated by the United States Environmental Protection Agency. The simulation is performed under city driving conditions. Fig. 11 shows the vehicle speed. With the ICE On/Off algorithm, ICE will be turned "On" when vehicle speed is higher than 37 km/h, and ICE turned "Off" when vehicle speed is lower than 33 km/h, as shown in Fig. 12.

TABLE III
VEHICLE DATA

ICE characteristics:	
Type	V6, SI engine
Engine volume (liter)	3.6
Peak torque (Nm)	300
Peak speed (rpm)	6000
EM characteristics:	
Type	Permanent magnet AC motors
Maximum power (kW)	60
Maximum speed (rpm)	10000
Peak efficiency	0.92
Peak torque (Nm)	190
Battery characteristics:	
type	Lithium-ion
Power (kW)	30
Transmission	
Type	Front wheel two-mode
Final ratio	3.02
Vehicle characteristic:	
Wheel radius (m)	0.352
Rolling resistance coef.	0.01
Vehicle front area (m^2)	2.642
Aerodynamic drag coef.	0.386
Total mass (kg)	1600

One advantage of the GM two-mode HEV is the capability to capture braking energy by both EMs. In the simulation, Fig. 13 shows that the initial SOC value was 0.55, and the SOC value at the end of the driving cycle was 0.5486. It meant that most energy taken from ESS to drive the vehicle was equal to the regenerative energy from MGs. Fig. 14 shows that both EMs can operate in motor mode or in generator mode. This control algorithm also improves the efficiency of the ICE. Fig. 15 shows that most ICE operating points had efficiency higher than 25% (BSFC 100 g/MJ). Comparing with the ICE operating points of conventional vehicle GM Impala 2013, shown in Fig. 16, the ICE of the HEV remains in the high efficiency region during the simulation. A comparison of fuel economy with a

conventional vehicle using the same ICE V6, 3.6l shows that the fuel economy of the two-mode HEV is 27.8% higher than that of conventional vehicle model. Table IV shows the fuel economy comparison.
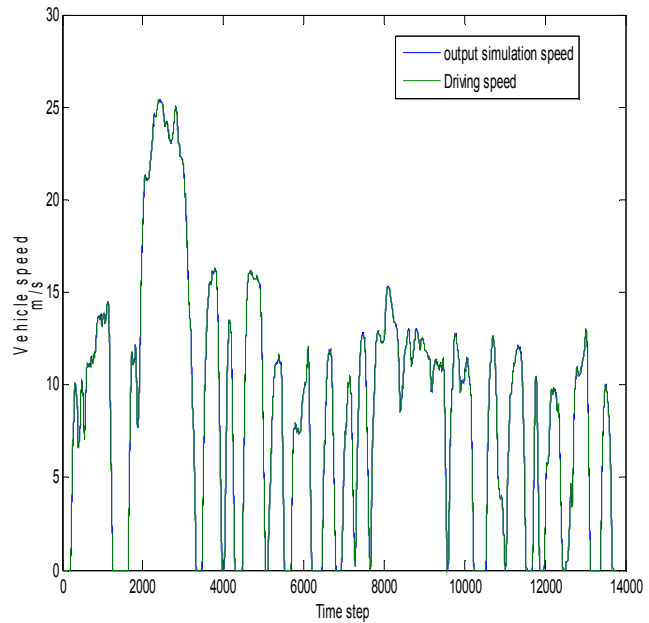

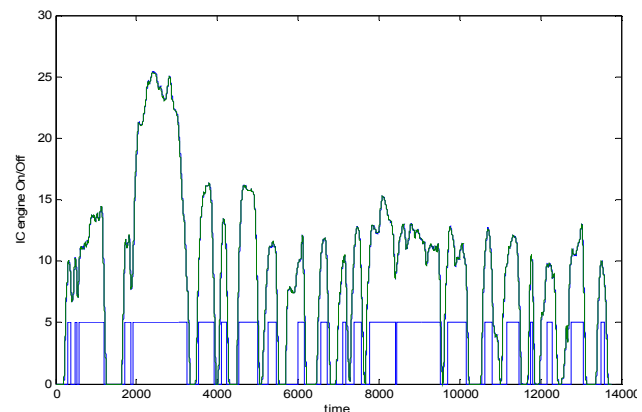Fig. 11 Vehicle speed tracking in UDDS driving cycle

Fig. 12 Engine On/Off status over UDDS driving cycle

V. CONCLUSIONS

This study compared simulations between a two-mode HEV model and a conventional vehicle. The input-split (EVT-1 mode) and compound-split (EVT-2 mode) both have critical operating ranges regarding the vehicle performance. At low vehicle speeds or at high acceleration rates, an input-split mode is used with high input/output ratio while the compound split gear set provides additional torque multiplication at high speed.
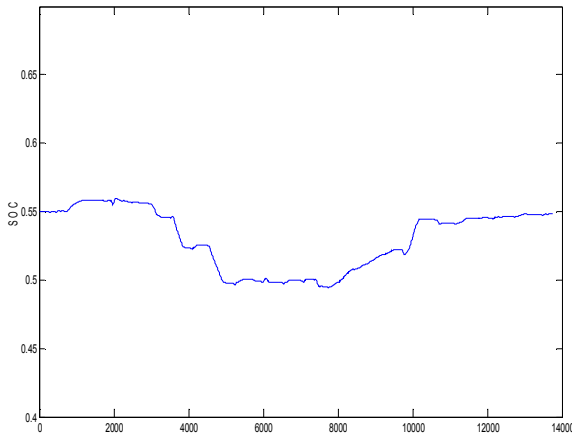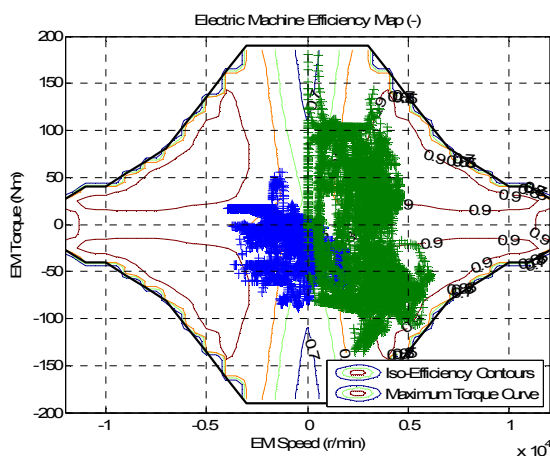
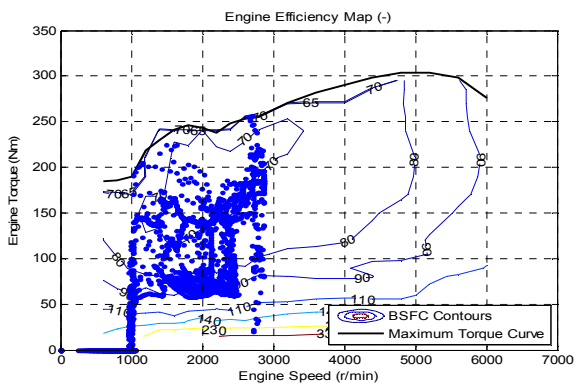Fig. 13 History of SOC

Fig. 14 EM operating points
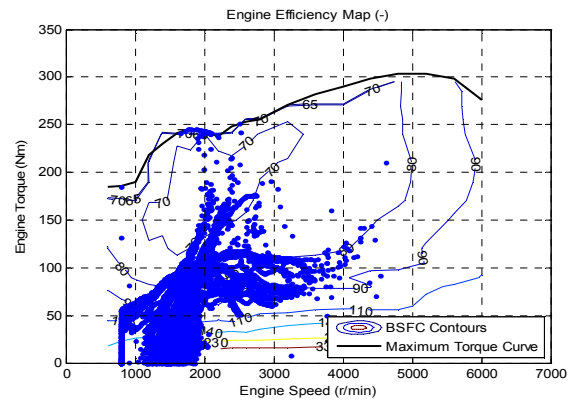

Fig. 15 ICE operating points of two-mode HEV

Fig. 16 ICE operating points of conventional vehicle (GM impala)

TABLE IV
FUEL ECONOMY COMPARISON BETWEEN GM TWO-MODE HYBRID AND
CONVENTIONAL GM IMPALA MODEL

Driving cycle	Conventional Vehicle Model	Two-mode HEV model	improvement
UDDS	21.64 mpg	27.67 mpg	27.8%

A fuzzy logic optimization can provide a quick and easy control method and is quickly and easily implemented to improve vehicle fuel economy. The simulation results show that the control strategy can satisfy driver demands, and ICE efficiency exceeds 22.7%. These improvements contribute to overall system efficiency, and the fuel economy of the HEV improves to 27.8% over that of conventional vehicle. The SOC of ESS is maintained in the optimal region.

REFERENCES

[1] R.T. Doucette, M.D. McCulloch, "Modeling the prospects of plug-in hybrid electric vehicles to reduce CO2 emissions," Appl. Energy, 88, 2315-2323, 2011.
[2] K.T. Chau, Y.S. Wong, "Overview of power management in hybrid electric vehicles," Energy Convers. Manage 43, 1953–1968, 2002.
[3] B. Wu, C.C. Lin, Z. Filipi, H. Peng, "Assanis, D. Optimal power management for a hydraulic hybrid delivery truck," Veh. Syst. Dyn, 42(1), 23–40, 2004.
[4] L. Wang, E.G. Collins Jr., H. Li, "Optimal design and real-time control for energy management in electric vehicles," IEEE Trans. Veh. Technol, 60(4), 1419-1429, 2011.
[5] J. Hendrickson, A. Holmes, D. Freiman, "General Motors front wheel drive two-mode hybrid transmission," SAE paper 2009-01-0508, 2009.
[6] T.M. Grewe, B.M. Conlon, A.G. Holmes, "Defining the General Motors 2-mode hybrid transmission," SAE paper 2007-01-0273, 2007.
[7] K. Ahn, S.W. Cha, "Developing mode shift strategies for a two-mode hybrid powertrain with fixed gears," SAE paper 2008-01-0307, 2008.
[8] G. Tamai, S. Reeves, T.H. Grewe, "Truck utility & functionality in the GM 2-mode hybrid," SAE paper 2010-01-0826, 2010.
[9] F.U. Syed, M.L. Kuang, J. Czubay, et al., "Derivation and experimental validation of a power-split hybrid electric vehicle model," IEEE Trans. on Vehicular Technology, 55, 1731-1747, 2006.
[10] Y. Gao, M. Ehsani, "A torque and speed coupling hybrid drivetrain - architecture, control, and simulation," IEEE Trans. on Power Electronics, 21, 741-748, 2006.

[11] C. Lin, Z. Filipi, Y. Wang, L. Louca, H. Peng, D. Assanis, J. Stein, "Integrated feed-forward hybrid electric vehicle simulation in SIMULINK and its use for power management studies," SAE Paper 2001-01-1334, 2001.

[12] C. Lin, H. Peng, J.W. Grizzle, J. Liu, M. Busdiecker, "Control system development for an advanced-technology medium-duty hybrid electric truck," SAE Paper 2001-01-3369, 2001.

[13] C. Lin, " Modeling and control strategy development for hybrid vehicles," Dissertation, P.H.D., University of Michigan, 2004.

[14] A. Piccolo, L. Ippolito, V. Galdi, A. Vaccaro, "Optimization of energy flow management in hybrid electric vehicles via genetic algorithms," Proceedings of 2001 IEEE/ASME International Conference on Advanced Intelligent Mechatronics, Como, Italy 2001.

[15] N. Schouten, M. Salman, N. Kheir, "Fuzzy logic control for parallel hybrid vehicles," IEEE Transactions on Control Systems Technology, 10(3), 460-468, 2002.

[16] F.R. Salmasi, "Control strategies for hybrid electric vehicles: evolution, classification, comparison, and future trends," IEEE Trans. on Vehicular Technology, 2393-2404, 2007.